Available online at www.sciencedirect.com
SCIENCE DIRECT®
Journal of Molecular Catalysis A: Chemical 222 (2004) 87–96
JOURNAL OF MOLECULAR CATALYSIS A: CHEMICAL
www.elsevier.com/locate/molcata

Gas-phase hydrogen transfer reduction of α,β-unsaturated ketones on Mg-based catalysts

J.I. Di Cosimo*, A. Acosta, C.R. Apesteguía

Catalysis Science and Engineering Research Group (GICIC), Instituto de Investigaciones en Catálisis y Petroquímica (INCAPE) (UNL-CONICET), Santiago del Estero 2654, (3000) Santa Fe, Argentina

Received 15 March 2004; received in revised form 26 July 2004; accepted 28 July 2004
Available online 9 September 2004

Abstract

The gas-phase regioselective reduction of mesityl oxide to the allyl alcohol using 2-propanol as a hydrogen donor was studied at 523 K on basic MgO, $MgAl_{0.33}O_x$ and $Cu_{0.05}MgAl_{0.65}O_x$ oxides. Catalysts were characterized using a variety of physical and spectroscopic techniques. The effect of contact time on the product distribution was determined in order to identify primary and secondary reaction pathways. Main reaction products from mesityl oxide conversion were the two allyl alcohol isomers (UOL, 4-methyl-3-penten-2-ol and 4-methyl-4-penten-2-ol), isomesityl oxide, methyl isobutyl ketone (MIBK), methyl isobutyl carbinol and C_9 aldol condensation products.

Bifunctional $Cu_{0.05}MgAl_{0.65}O_x$ did not produce alcohols. Metallic Cu atoms readily decomposed 2-propanol forming acetone and mobile surface H atoms that selectively reduced the C=C bond of mesityl oxide giving mainly MIBK.

UOL formed on MgO at unusually high yields for a gas-phase reaction (40% at 523 K, 2-propanol/mesityl oxide = 5 and HLSV = 14 $cm^3/(h\,g)$). UOL formation on MgO proceeds via a hydrogen transfer Meerwein–Ponndorf–Verley (MPV) mechanism without participation of surface H atoms from 2-propanol dissociation. Weak acid–strong base Mg^{2+}–O^{2-} surface pairs efficiently promote formation of the six-atom cyclic intermediate required in the MPV mechanism for selectively reducing the C=O bond of an unsaturated ketone to the corresponding allyl alcohol.

In contrast, UOL yield on $MgAl_{0.33}O_x$ was always lower than 5%. UOL formation is hindered on $MgAl_{0.33}O_x$ because surface Al^{3+} sites decrease by dilution the density of Mg^{2+}–O^{2-} pairs and concomitantly favor the adsorption of mesityl oxide via the C=C bond, thereby promoting the selective formation of MIBK.

Keywords: Regioselectivity; Hydrogen transfer; Basic catalysis; α,β-Unsaturated ketones; Reduction

1. Introduction

Among the reduction processes of carbonyl-containing unsaturated compounds, those that selectively reduce the carbonyl group preserving the other functional groups in the molecule are of special interest in fine chemical synthesis. These regioselective processes have been extensively studied in liquid phase under high hydrogen pressures on both supported noble metal catalysts and non-noble mixed oxide catalysts [1,2]. The carbonyl function of unsaturated aldehydes is more easily reduced as compared to that of unsaturated ketones [3,4]. Actually, the selective hydrogenation of unsaturated ketones by molecular hydrogen toward the corresponding allyl alcohols with high yields was only recently reported [5,6].

The hydrogen transfer reduction (HTR) of aldehydes and ketones provides a highly selective alternative route for alcohol synthesis. In the HTR reaction, the carbonyl compound (oxidant) is contacted with a hydrogen donor reactant (reductant) at mild conditions in liquid or gas phase thereby avoiding the use of pressurized hydrogen. This redox reaction

* Corresponding author. Tel.: +54 342 4555279; fax: +54 342 4531068.
E-mail address: dicosimo@fiqus.unl.edu.ar (J.I.D. Cosimo).

1381-1169/$ – see front matter © 2004 Elsevier B.V. All rights reserved.
doi:10.1016/j.molcata.2004.07.020

can be depicted as Eq. (1):

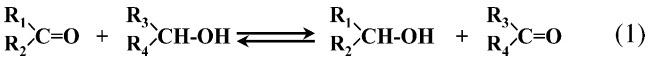

(1)

where a hydride is transferred from the alcohol to the carbonyl compound with no involvement of molecular hydrogen.

It is generally accepted that HTR of aldehydes and ketones on oxides occurs via a Meerwein–Ponndorf–Verley (MPV) mechanism which involves the selective hydrogenation of the C=O bond leaving unreacted the other reducible functional groups of the reactant molecule [3,7]. Recently, several regio, chemo, enantio or stereoselective applications of the HTR reaction have been reported [7–10] either in liquid or in gas phases using solid catalysts. Zeolites and metal oxide catalysts containing Lewis acid or base surface sites have been shown to promote HTR reaction [7,11,12]. The reaction mechanism, the occurrence of side reactions, and the catalyst activity decay strongly depend on the acid–base nature of the catalyst. For example, acidic catalysts frequently dehydrate the obtained alcohol forming olefins, whereas basic catalysts promote consecutive aldol condensations of the carbonyl intermediates.

Most of the contributions on HTR reaction applications lately reported deal with the reduction of saturated carbonyl compounds and very few with unsaturated ketones or aldehydes. However, the HTR reaction is particularly suitable for the reduction of α,β-unsaturated carbonyl compounds to the corresponding allyl alcohols since the C=C bond is not affected. In fine chemistry applications, the allyl alcohol is usually the most valuable and difficult to obtain product of the α,β-unsaturated carbonyl reduction [9] because the reaction generally proceeds further toward formation of saturated carbonyl or alcohol compounds.

Gas-phase reduction of unsaturated carbonyl compounds such as cinnamaldehyde, citral, acrolein, 4-hexen-3-one, cyclohexenone or 5-hexen-2-one to the corresponding unsaturated alcohols has been explored in the literature with diverse level of success using Mg-based catalysts, such as MgO, Mg–B, or Mg–Al mixed oxides in flow reactors. Allyl alcohol yields of 4–88% were achieved within a wide range of operating conditions, i.e. temperatures between 473 and 723 K, alcohol/carbonyl molar ratio of 2–20, and HLSV of 0.6–2500 cm^3 of liquid reactant/(h g-catalyst) [8,13–16].

In this paper, we study the gas-phase reduction of mesityl oxide, an α,β-unsaturated ketone, toward the allyl alcohol (4-methyl-3-penten-2-ol), by HTR using 2-propanol as a hydrogen donor on acid–base and bifunctional metal/acid–base catalysts according to Eq. (2), where acetone is the product of the 2-propanol oxidation. Specifically, we first prepared and characterized Mg-based catalysts such as MgO, Mg–Al and Mg–Al–Cu mixed oxides, and then determined their catalytic performance. Results show a distinct catalytic behavior for each catalyst formulation that is interpreted in terms of the role played by the different surface species (acid–base or metallic) in the coordination of the carbonyl group for regioselective allyl alcohol formation. We identify primary and secondary pathways involved in mesityl oxide reduction mechanism by modifying the contact time. We also discuss the effect of varying the reaction atmosphere on the activity and product distribution of this reaction. Our goal was to elucidate the reaction pathways leading to allyl alcohol and saturated compounds and to ascertain the nature of the surface species that promote these reactions.

2. Experimental

2.1. Catalyst synthesis

Mg–Al and Cu–Mg–Al mixed oxides identified as $(Cu_y)MgAl_zO_x$ were prepared by co-precipitation method at a constant pH of 10 following similar procedures. For the ternary Cu–Mg–Al catalyst, a nitrate solution with a total [Mg + Al + Cu] cation concentration of 1.5 M was contacted with a basic solution of K_2CO_3 and KOH by dropwise addition of both solutions into a stirred beaker containing 350 cm^3 of distilled deionized water held at 333 K. The precipitates formed were aged in their mother liquor for 2 h at 333 K and then filtered, washed with boiling distilled water until K^+ was no longer detected in the filtrate, and dried at 348 K overnight. Dried precursors were decomposed in N_2 or air at 773 K overnight in order to obtain the corresponding $(Cu_y)MgAl_zO_x$ samples. High surface area pure MgO was prepared by hydration with distilled water at room temperature of commercial MgO (Carlo Erba, 99%, 27 m^2/g) and further decomposition in N_2 at 773 K. Details are given elsewhere [17].

In addition, a Cu/SiO_2 (SiO_2, Grace 62, 99.7%) sample was prepared by incipient wetness impregnation by dropwise addition of an aqueous solution of $Cu(NO_3)_2{\cdot}3H_2O$ with a copper concentration of 0.6 M. After drying, sample was calcined in air at 773 K overnight.

2.2. Catalyst characterization

The crystalline phases in the coprecipitates and in the mixed oxides were determined by X-ray diffraction (XRD) using a Shimadzu XD-D1 diffractometer and Ni-filtered Cu Kα radiation. Crystallite sizes were calculated from the CuO (1 1 1) diffraction lines using the Scherrer equation.

The total CO_2 adsorption site densities and binding energies were obtained from temperature-programmed desorption (TPD) of CO_2 preadsorbed at room temperature.

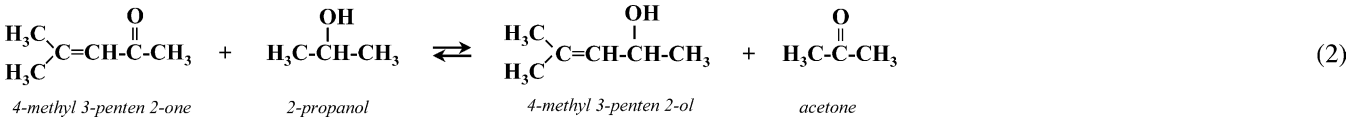

(2)

4-methyl 3-penten 2-one *2-propanol* *4-methyl 3-penten 2-ol* *acetone*

Samples (150 mg) were pretreated in N_2 at 773 K for 1 h and then exposed to a flow of 100 cm^3/min of 3.09% CO_2/N_2 at room temperature until saturation coverage was reached. Weakly adsorbed CO_2 was removed by flowing N_2 and then the temperature was increased to 773 K at 10 K/min. The evolved CO_2 was converted to methane by means of a methanation catalyst (Ni/Kieselghur) operating at 673 K and monitored using a flame ionization detector.

BET surface areas (*Sg*) were measured by N_2 physisorption at its boiling point using a Quantachrome Nova-1000 sorptometer. Bulk elemental analysis of Cu, Mg, Al and K was carried out by atomic absorption spectroscopy (AAS).

2.3. Catalytic testing

Catalytic tests were conducted at 523 K and atmospheric pressure in a fixed bed reactor. Samples sieved at 0.35–0.42 mm were pretreated in N_2 at 773 K for 1 h before reaction in order to remove adsorbed H_2O and CO_2. In addition, Cu-containing catalysts were reduced in situ in flowing H_2 at 573 K for 1 h prior the catalytic test.

The reactants, mesityl oxide, MO (Acros 99%, isomer mixture of mesityl oxide/isomesityl oxide = 91/9) and 2-propanol, 2P (Merck, ACS, 99.5%) were introduced as a mixture with the proper molar composition via a syringe pump and vaporized into flowing N_2 or H_2 to give a $N_2(H_2)$/2-propanol = 12 (molar). The hourly liquid space velocity (HLSV) of the reactant mixture was varied in the range of 14–400 cm^3/(h g-cat.). Reaction products were analyzed by on-line gas chromatography in a Varian Star 3400 CX chromatograph equipped with a flame ionization detector and a 0.2% Carbowax 1500/80–100 Carbopack C column. Main reaction products from MO conversion were identified as the two unsaturated alcohol isomers (UOL, 4-methyl-3-penten-2ol and 4-methyl-4-penten-2ol), isomesityl oxide (*i*-MO), methyl isobutyl ketone (MIBK) and methyl isobutyl carbinol (MIBC). At high MO conversion levels, C_9 oxygenates such as diisobutyl ketone (DIBK), diisobutyl carbinol (DIBC) and phorones were also obtained as well as other unidentified heavier condensation products (C_{9+}). The total C_9 aldol condensation products (DIBK + DIBC + phorones) are identified in the text as AC. Acetone (DMK) was produced by 2P oxidation in HTR reaction (Eq. (2)). Small amounts of C_3 hydrocarbons (propane or propylene) were formed by 2P dehydration. Selectivities (S_i, carbon atoms of product *i*/carbon atoms of MO reacted) and yields (η_i, carbon atoms of product *i*/carbon atoms of MO fed) were calculated as $S_i = F_i N_i / \sum F_i N_i$ and $\eta_i = F_i N_i / 6F^0_{MO}$, where F_i is the molar flow of a product *i* formed from MO, N_i the number of carbon atoms in product *i* and F^0_{MO} the molar flow of MO in the feed. Due to catalyst deactivation, the catalytic results reported here were calculated by extrapolation of the reactant and product concentration curves to zero time on stream. Then, *X*, *S*, and η represent conversion, selectivity, and yield at $t = 0$, respectively.

3. Results and discussion

3.1. Characterization

The chemical composition, BET surface area, and crystalline phases of mixed oxides and MgO are shown in Table 1. Elemental analysis of the oxides revealed that the actual composition was very similar to the nominal one, suggesting complete precipitation of Mg and Al or Cu salts during synthesis. The potassium content in all the mixed oxides was below 0.1 wt.%, which confirms that K^+ ions were effectively removed by washing of the precipitated precursors.

X-ray diffraction pattern for Cu/SiO_2 exhibited a single well-defined CuO phase; calculations showed that on this sample the CuO crystallite size was about 250 Å. The diffraction patterns of $MgAl_{0.33}O_x$ and of unreduced $Cu_{0.05}MgAl_{0.65}O_x$ mixed oxides showed broad XRD lines corresponding to a quasi-amorphous MgO periclase phase, probably because the hydrated precursors were decomposed at relatively low temperatures (773 K). $Cu_{0.05}MgAl_{0.65}O_x$ contained an additional $MgAl_2O_4$ spinel phase and copper oxide (CuO, tenorite), which was detected as a poorly crystalline phase, thereby suggesting that in $Cu_{0.05}MgAl_{0.65}O_x$ sample copper is highly dispersed in the mixed oxide matrix.

In previous work [18–20], we characterized the surface basicity of similar Mg-based catalysts by using a combination of spectroscopic techniques and identified three different surface basic sites. We also determined the following base strength order for these sites: low coordination O^{2-} anions > oxygen in Mg^{2+}–O^{2-} pairs > OH^- groups. In the present

Table 1
Catalyst physicochemical properties

Catalyst	*Sg* (m^2/g)	Phases detected[a]	Base site density[b] (μmol/m^2)	Chemical composition[c] (wt.%)		
				Mg	Al	Cu
MgO	136	MgO periclase	5.6	60.3	–	–
$MgAl_{0.33}O_x$	200	MgO periclase	3.3	34.4	12.1	–
$Cu_{0.05}MgAl_{0.65}O_x$	245	MgO, $MgAl_2O_4$, CuO[d]	1.4	31.4	22.7	4.0
Cu/SiO_2	233	CuO	0.0	–	–	6.1

[a] By XRD.
[b] By TPD of CO_2.
[c] By AAS.
[d] Traces.

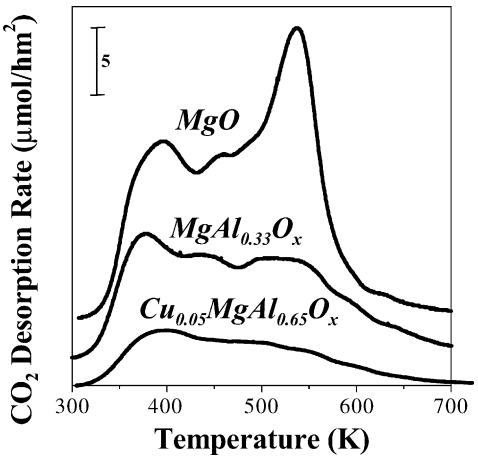

Fig. 1. CO_2 TPD traces of basic Mg-based catalysts.

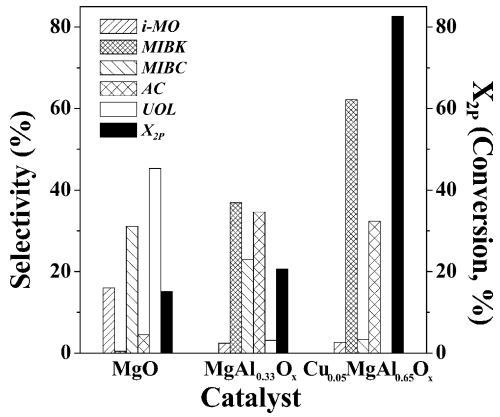

Fig. 2. Selectivities and conversions at $t = 0$ on different Mg-based catalysts for gas-phase HTR of MO with 2P. $T = 523$ K; $P_T = 100$ kPa; N_2/2P/MO = 93.4/6.6/1.3 kPa; $X_{MO} = 85$–89%.

work, we have measured CO_2 adsorption site densities and binding energies by TPD of CO_2. The CO_2 desorption rate as a function of sample temperature is presented in Fig. 1 for MgO, $MgAl_{0.33}O_x$ and $Cu_{0.05}MgAl_{0.65}O_x$ samples. The total amount of desorbed CO_2 was measured by integration of TPD curves. The resulting values are reported in Table 1.

The base site density and strength distribution depended on the acid–base properties of the metal cations present in the catalyst formulation. In mixed oxides containing Lewis acidic cations such as $MgAl_{0.33}O_x$ and $Cu_{0.05}MgAl_{0.65}O_x$, the base site density is lower than in MgO. Just 12.1 wt.% Al in the catalyst formulation of $MgAl_{0.33}O_x$ decreased the base site density by almost a factor of 2 compared to pure MgO. On the other hand, the number of surface basic sites on Cu/SiO_2 was negligible.

Similarly, the TPD traces of Fig. 1 show that the binding energies of adsorbed CO_2 species are affected by the electronegativity of the metal cations. MgO contains not only weak (CO_2 desorption temperature ≈400 K) and medium-strength (≈450 K) but also high-strength base sites (≈550 K). In general, the amount of strong base sites decreased with increasing the catalyst Al content. Catalyst $Cu_{0.05}MgAl_{0.65}O_x$ presents a low total density of base sites and almost no high-strength base sites.

3.2. Catalyst activity and selectivity

Catalyst activity and selectivity for the HTR of MO with 2P were investigated by carrying out catalytic experiments at similar MO conversion levels (X_{MO} = 85–89%). Fig. 2 compares the catalyst performance at 523 K resulting from contacting the catalyst bed with the reactant mixture previously vaporized in N_2 (N_2/2P/MO = 93.4/6.6/1.3 kPa).

For a reactant mixture of 2P/MO = 5 molar ratio, the expected X_{MO}/X_{2P} conversion ratio should be 5, either if stoichiometric selective reduction of C=O (Eq. (2)) or C=C (Eq. (3)) double bonds of MO takes place.

$$MO + 2P \rightleftarrows MIBK + DMK \quad (3)$$

2P conversion (X_{2P}) was 15% on MgO and 20% on $MgAl_{0.33}O_x$, giving in both cases a X_{MO}/X_{2P} conversion ratio close to 5, what suggests that a HTR reaction predominates. In contrast, on $Cu_{0.05}MgAl_{0.65}O_x$ catalyst, 2P conversion reached a value of 83% ($X_{MO}/X_{2P} \approx 1$), thereby indicating that 2P participates in other reactions besides HTR.

Metallic copper is industrially used in acetone synthesis from 2-propanol [21] because its well known dehydrogenating properties. Furthermore, we have previously demonstrated that Cu^0/acid–base catalysts are about 1000 times more active to dehydrogenate 2P than Cu-free acid–base catalysts [18]. Thus, the high 2P conversion observed on $Cu_{0.05}MgAl_{0.65}O_x$ catalyst is attributed to the fact that surface Cu^0 atoms readily convert 2P in DMK and molecular hydrogen.

Fig. 2 also shows the product distribution on MgO, $MgAl_{0.33}O_x$, and $Cu_{0.05}MgAl_{0.65}O_x$ samples. On MgO, selectivity to UOL was 45% (38% of 4-methyl-3-penten-2-ol and 7% of 4-methyl-4-penten-2-ol); other unsaturated compounds such as *i*-MO (16%) and AC products (4.5% phorones) were also obtained. Phorones are C_9 unsaturated ketones formed by aldol condensation of MO with the DMK resulting from 2P oxidation. The saturated alcohol, MIBC, was obtained with 31% selectivity, whereas the saturated ketone, MIBK, was detected only in negligible amounts. Formation of the MO isomer, *i*-MO, is explained by C=C double bond isomerization of MO. Similarly to isomerization of olefins on basic oxides, this reaction proceeds via carbanion intermediates [22] as depicted in Scheme 1. Although the isomerization reaction involves formation of mobile surface protons, not necessarily incorporates hydrogen from the hydrogen donor as it may proceed by intramolecular hydrogen transfer. In the same way, formation of 4-methyl-4-penten-2-ol, can be assigned to fast C=C double bond isomerization of 4-methyl-3-penten-2-ol, the unsaturated alcohol resulting from C=O reduction of MO or to C=O reduction of *i*-MO.

On $MgAl_{0.33}O_x$ mixed oxide, formation of the unsaturated compounds (UOL and *i*-MO) was almost completely

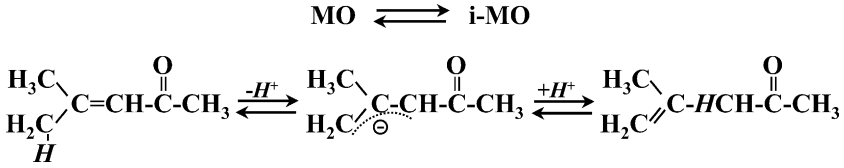

Scheme 1. Double bond isomerization of MO.

suppressed. Contrarily, the selectivity to saturated compounds raised significantly up to 60% (37% MIBK and 23% MIBC) compared to MgO. Selectivity to AC compounds also increased drastically to 34% but in contrast to MgO, $MgAl_{0.33}O_x$ formed saturated aldol condensation products (10% DIBK and 24% DIBC). DIBK and DIBC formed by cross-aldol condensation of MO or MIBK with DMK, followed by fast dehydration of the aldol intermediate and consecutive HTR of the C_9 α,β-unsaturated product. These results suggest that the $MgAl_{0.33}O_x$ catalyst combines metal cations of different electronegativities which promote both C=C and C=O reductions giving mainly C_6 and C_9 saturated ketones and alcohols.

$Cu_{0.05}MgAl_{0.65}O_x$ produced MIBK (62%) and AC compounds (32% DIBK and 0.8% phorones), but neither form UOL nor DIBC and yielded only small amounts of MIBC. In addition to the acid–base sites, $Cu_{0.05}MgAl_{0.65}O_x$ catalyst contains surface Cu^0 atoms. The role of the Cu^0 atoms on the selectivity of HTR reactions was explored by carrying out additional catalytic runs on a 6 wt.% Cu/SiO_2 sample. The selectivity to MIBK on Cu/SiO_2 was about 95%, thereby suggesting that copper (Table 2), supported on inert solids promotes almost exclusively the C=C bond hydrogenation of MO molecule. Similar findings on Cu/SiO_2 have been reported by Ravasio et al. [23] in the liquid-phase hydrogenation of other α,β-unsaturated ketones. Since the Cu/SiO_2 catalyst did not promote aldol condensations reactions, formation of AC compounds on $Cu_{0.05}MgAl_{0.65}O_x$ must be attributed to the surface acid–base properties of this sample. In $Cu_{0.05}MgAl_{0.65}O_x$ catalyst, copper metal atoms are better dispersed than in the silica matrix thereby favoring the interaction between metal and acid–base sites. The bifunctional catalysis operating on $Cu_{0.05}MgAl_{0.65}O_x$ explains why this sample, in contrast to $MgAl_{0.33}O_x$, produces only C_6 and C_9 ketones.

3.3. Effect of contact time: reaction pathways

The effect of contact time (W/F^0_{MO} and W/F^0_{2P}) on the product distribution was determined in order to identify primary and secondary reaction pathways. The observed deactivation, however, required that each data point be obtained on a fresh catalyst and that product yields (η_i) and conversions (X_{MO} and X_{2P}) be obtained by extrapolating to zero time on stream using proper fitting functions. Figs. 3–5 show the results obtained at 523 K on $Cu_{0.05}MgAl_{0.65}O_x$, $MgAl_{0.33}O_x$, and MgO, respectively, using a 2P/MO = 5 reactant molar ratio and a wide contact time range (W/F^0_{MO} = 1.5–42.0 g-cat. h/mol MO; W/F^0_{2P} = 0.3–8.4 g-cat. h/mol 2P). From the initial slopes of the X_{MO} and X_{2P} versus W/F^0_{MO} curves and from those of the η_i versus W/F^0_{MO} plots, the areal initial conversion rate of each reactant (r^0_{MO} and r^0_{2P}) and the areal initial formation rates of product i (r^0_i) were calculated according to

$$r^0_{MO} = \frac{1}{Sg}\left[\frac{dX_{MO}}{d(W/F^0_{MO})}\right]_{W/F^0_{MO}=0}$$

$$r^0_{2P} = \frac{1}{Sg}\left[\frac{dX_{2P}}{d(W/F^0_{2P})}\right]_{W/F^0_{2P}=0} = \frac{5}{Sg}\left[\frac{dX_{2P}}{d(W/F^0_{MO})}\right]_{W/F^0_{MO}=0}$$

$$r^0_i = \frac{1}{Sg}\left[\frac{d\eta_i}{d(W/F^0_{MO})}\right]_{W/F^0_{MO}=0}$$

as presented in Table 2.

Calculations for Eq. (2) using additivity rules for the estimation of thermodynamic parameters [24] led us to conclude that unsaturated alcohol formation by gas-phase HTR of MO with 2P at 523 K is a slightly endothermic process favored at high 2P/MO ratios. At 523 K and 2P/MO = 5, the

Table 2
Gas-phase HTR of mesityl oxide with 2-propanol

Catalyst	Initial conversion rates (μmol/(h m²))		Initial formation rates (μmol/(h m²))		
	r^0_{MO}	r^0_{2P}	r^0_{UOL} (C=O)	r^0_{MIBK} (C=C)	r^0_{MIBC} (C=O + C=C)
MgO	711	992	182	9	146
MgO[a]	–	14	–	–	–
$MgAl_{0.33}O_x$	785	800	47	296	69
$Cu_{0.05}MgAl_{0.65}O_x$	1011	2225	29	683	132
Cu/SiO_2	382	270	4	363	5

T = 523 K; N_2/2P/MO = 93.4/6.6/1.3 kPa.
[a] N_2/2P = 93.5/7.8 kPa.

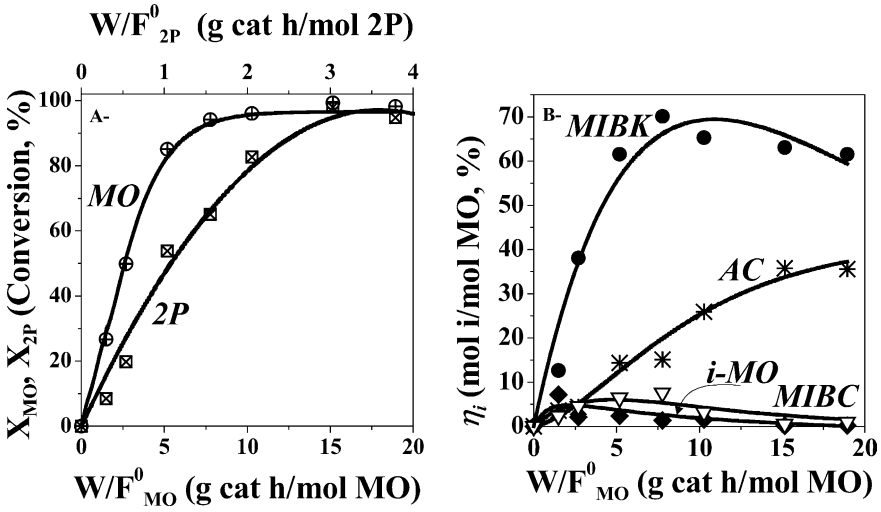

Fig. 3. Gas-phase HTR of MO with 2P on $Cu_{0.05}MgAl_{0.65}O_x$. (A) Reactant conversions at $t = 0$; (B) product yields at $t = 0$. $T = 523$ K; $P_T = 100$ kPa; N_2/2P/MO = 93.4/6.6/1.3 kPa.

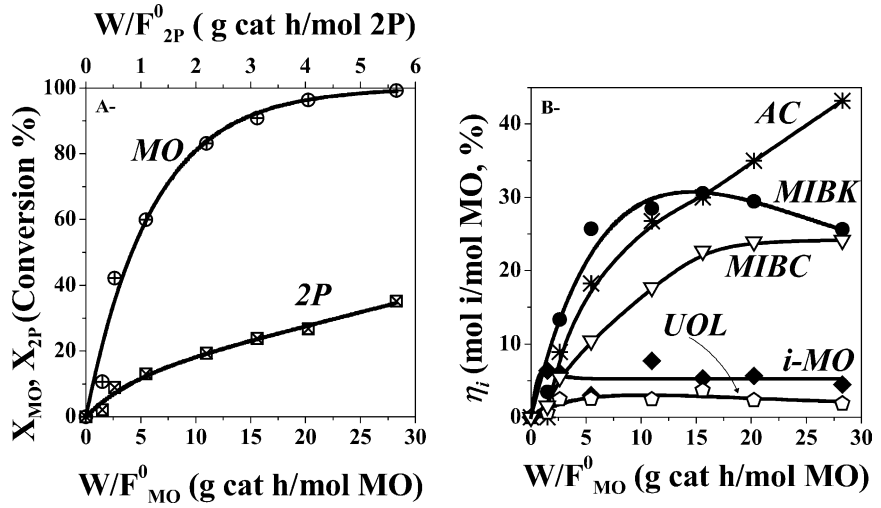

Fig. 4. Gas-phase HTR of MO with 2P on $MgAl_{0.33}O_x$. (A) Reactant conversions at $t = 0$; (B) product yields at $t = 0$. $T = 523$ K; $P_T = 100$ kPa; N_2/2P/MO = 93.4/6.6/1.3 kPa.

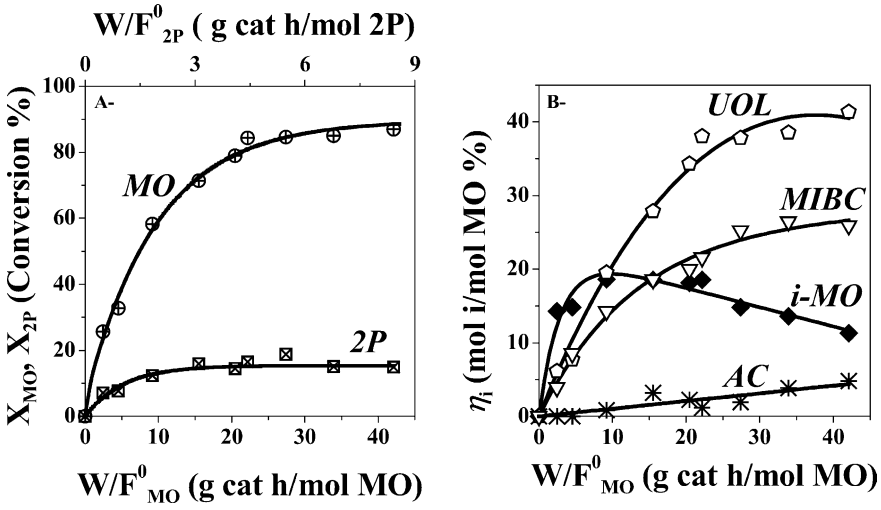

Fig. 5. Gas-phase HTR of MO with 2P on MgO. (A) Reactant conversions at $t = 0$; (B) product yields at $t = 0$. $T = 523$ K; $P_T = 100$ kPa; N_2/2P/MO = 93.4/6.6/1.3 kPa.

calculated MO and 2P equilibrium conversions were 80 and 16%, respectively. However, the experimental MO and 2P conversions were in general higher than those values because of consecutive or parallel reactions. Nevertheless, at all contact times C_3 hydrocarbons were observed in negligible amounts on the three catalysts, thereby confirming that 2P molecules do not participate significatively in dehydration reactions.

On bifunctional $Cu_{0.05}MgAl_{0.65}O_x$ catalyst, we measured MO and 2P conversions of up to 100% (Fig. 3A). The main and primary product is MIBK, as indicated in Fig. 3B by its non-zero initial slope; MIBK converts to AC products at increasing contact times. MIBC yield is low on $Cu_{0.05}MgAl_{0.65}O_x$ over the entire contact time range studied because consecutive MIBK reduction to MIBC with H fragments formed by 2P decomposition on Cu^0 is thermodynamically unfavored [24]. Formation of UOL was detected only at very short contact times, but in yields lower than 1%.

MO and 2P conversions of up to 100 and 35%, respectively, were achieved on the slightly acidic $MgAl_{0.33}O_x$ mixed oxide (Fig. 4A). On this catalyst, UOL is a primary product but η_{UOL} was lower than 5% in all the conversion range, as shown in Fig. 4B. The main reaction pathway leads to primary MIBK formed by direct reduction of the C=C bond of MO. MIBK reaches a maximum concentration as it rapidly converts to larger oxygenates in secondary condensation reactions (AC compounds) with increasing contact time. MIBC is probably formed at short contact times by fast consecutive HTR of MIBK with 2P. At high contact times, aldol condensation reactions clearly prevail over the HTR reactions.

The highest MO conversion measured on MgO (Fig. 5A) was 87%. On the strongly basic MgO, UOL is a primary product formed directly from MO or *i*-MO as indicated by its non-zero initial slope in Fig. 5B. UOL yield increases monotonically with increasing contact time because on MgO the consecutive conversion of UOL to secondary products is not favored, in contrast to what is usually observed in liquid-phase on noble metal catalysts, on which the allyl alcohol is rapidly isomerised to the saturated ketone via enol formation [25] or further hydrogenated to the saturated alcohol [26]. MIBK yields of <1% were measured at increasing contact times. Consequently, UOL is the main reaction product on MgO at high contact times. Similarly, *i*-MO is a primary product that is probably converted into UOL at higher contact times.

The initial slope of the MIBC curve in Fig. 5B suggests that this product forms directly from the MO and 2P reactants, as depicted in Eq. (4). This reaction is highly exothermic with an equilibrium constant 10^6 times higher than that of UOL formation according to Eq. (2). At high contact times, MIBC is also formed by consecutive HTR from *i*-MO. Finally, the initial zero slope for AC formation reveals that this product is produced via the consecutive condensation of primary products.

$$MO + 2(2P) \rightleftarrows MIBC + 2\,DMK \quad (4)$$

3.4. Surface properties and catalytic performance

The distinct catalytic behavior observed on $Cu_{0.05}MgAl_{0.65}O_x$, $MgAl_{0.33}O_x$, and MgO samples may be explained by considering essentially the role played by the different surface species (acid–base or metallic sites) on both the coordination of reactant molecules and the selective promotion of C=C or C=O bonds in the adsorbed MO molecule.

On MgO, HTR reaction proceeds by a Meerwein–Ponndorf–Verley (MPV) mechanism. Traditionally, the MPV reaction was a homogeneous process catalyzed by metal alkoxides with participation of a Lewis acid center. The reaction mechanism of the homogeneous reaction involves formation of a cyclic six-membered intermediate in which both reactants are coordinated to the metal of the alkoxide [7]. It is customary to postulate a similar intermediate for the heterogeneously catalyzed process, as presented in Scheme 2, in which MO adsorption takes place via the C=O bond on a weak Lewis acid Mg^{2+} cation, whereas 2P adsorbs non-dissociatively on a vicinal Mg^{2+}–O^{2-} pair, giving rise to a cyclic six-atom surface intermediate. Thus, in the MPV concerted mechanism, the hydride transfer (H^{α}) occurs selectively toward allyl alcohol formation without participation of surface H fragments from alcohol dissociation. It has been debated in the literature whether the ketone adsorbs on a Lewis acid cation [27,28] or on an OH group generated from alcohol adsorption [12]. The MO adsorption on the Mg^{2+} cations as we postulate in Scheme 2 for the gas-phase allyl alcohol synthesis is supported by the presence of phorones among the reaction products. Formation of phorones by aldol condensation requires, in fact, initial activation of the reactant ketones (MO and DMK) on vicinal Lewis acid sites, as postulated previously for similar aldolization reactions [29]. Besides, strong MO adsorption on MgO probably impedes further UOL competitive adsorption, thereby preventing consecutive transformation of UOL to secondary products by releasing the UOL molecule to the gas phase. This is consistent with the fact that UOL is the main reaction product at high conversions.

Formation of MIBK on MgO via the initial reduction of the C=C bond of MO is very low, but significant amounts of MIBC are produced. Table 2 shows that r^0_{MIBC} is more than one order of magnitude higher than r^0_{MIBK}. Therefore, the unselective reduction of MO to MIBC can be envisaged as occurring according to Eq. (4), probably by a simultaneous

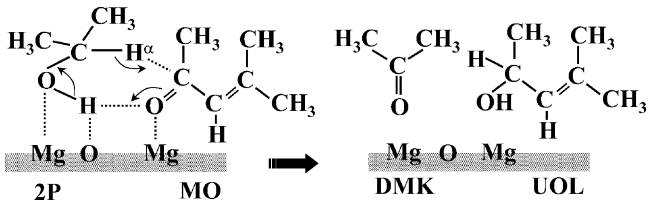

Scheme 2. Gas-phase HTR of MO with 2P on MgO. Allyl alcohol formation by MPV mechanism.

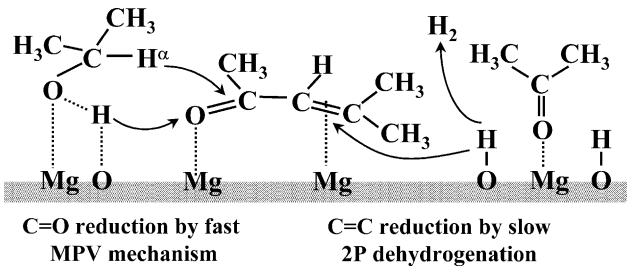

Scheme 3. Gas-phase HTR of MO with 2P on MgO. MIBC formation.

di-π adsorption mode of both C=C and C=O bonds [4,30] or by "on top" combined with π_{C-C} adsorption modes on the Mg^{2+} cations as sketched in Scheme 3. However, reduction of the C=C bond cannot be achieved by direct hydrogen transfer from 2P as in the MPV mechanism, and thus dissociative 2P adsorption with formation of hydrogen and DMK might supply the surface H fragments. Participation of surface H fragments in reduction of the C=C bond of MO on MgO, was confirmed by performing catalytic tests in H_2 atmosphere. In fact, MIBK was observed in significant concentrations all along the catalytic run and the MIBK/MIBC selectivity ratio clearly increased by an order of magnitude when gas phase hydrogen was included in the reactant feed (Table 3).

Additional 2P dehydrogenation experiments carried out by injecting 2-propanol diluted in N_2 on MgO (Table 2) indicated that this reaction is significantly slower (r^0_{2P} = 14 μmol/(h m^2)) compared with UOL formation by MPV mechanism (r^0_{UOL} = 182 μmol/(h m^2)). Thus, the hydrogen transfer rate from 2P to MO via a MPV mechanism on MgO is more rapid than the formation of H fragments by 2P dehydrogenation to DMK. This result explains why the formation of UOL (Scheme 2) is kinetically favored compared to the formation of MIBC (Scheme 3).

Contrarily to what was found on MgO, MIBK was initially formed at high rates on $MgAl_{0.33}O_x$ (r^0_{MIBK} = 296 μmol/(h m^2)). This is explained by considering that the presence of Al^{3+} cations in the catalyst gives rise to two possible mechanisms leading to selective hydrogenation of MO to MIBK: (i) Michael addition of a hydride (H^α of the adsorbed 2-propoxide intermediate) to the C_4 atom of adsorbed MO (C=C bond) followed by protonation of the resulting carbanion at the C_3 carbon atom of MO; (ii) adsorption of MO via a π_{C-C} complex of the C=C bond on the Al^{3+} cations, which are stronger Lewis acid sites than Mg^{2+} (Scheme 4). Both mechanisms imply formation of surface hydrogen fragments from 2-propanol dissociation and at the present we have no means to ascertain which one contributes the most to MIBK formation.

As stated above for MgO, reduction of the C=C bond on $MgAl_{0.33}O_x$ would require hydrogen fragments to be present on the surface. In previous work [20], we studied 2-propanol dehydrogenation on MgO and Mg–Al mixed oxides and found that the former is a better dehydrogenating catalyst. The dehydrogenation rate of 2P on a $MgAl_{0.33}O_x$ catalyst at 533 K was three times slower than on MgO but not negligible. Thus, participation of the Al^{3+} in providing the H fragments for C=C reduction cannot be excluded, even though they are not considered in Scheme 4. Involvement of surface H fragments in reduction of the C=C bond of MO on $MgAl_{0.33}O_x$ was confirmed by comparing catalytic tests in N_2 and in H_2 atmosphere (Table 3). A slight increase of the MIBK/MIBC selectivity ratio was observed in H_2. The smaller increment compared to that measured on MgO is explained by the fact that Mg–Al mixed oxides are less active than MgO to promote H_2 dissociation [29].

Once the saturated ketone (MIBK) has formed on $MgAl_{0.33}O_x$, it readily converts to MIBC by a MPV mechanism probably involving both Mg^{2+} and Al^{3+} surface sites (Scheme 4). Mg–Al mixed oxides have been reported as very active and selective catalysts for HTR of saturated ketones toward the saturated alcohol [31,32]. In particular, Jyothi et al. [13] reported a 95% MIBC yield in the gas-phase HTR of MIBK with 2P at 473 K and low HLSV (1.5 cm^3/(h g-cat.)) on a $MgAl_{0.33}O_x$ mixed oxide. However, Mg–Al mixed oxides are not selective for the HTR of unsaturated ketones toward the unsaturated alcohol (Table 2).

Although UOL is a primary product on $MgAl_{0.33}O_x$ (Fig. 4B), UOL synthesis is hampered on this catalyst (r^0_{UOL} = 47 μmol/(h m^2)) irrespective of the conversion level, probably because surface Al^{3+} sites decrease by dilution the density of Mg^{2+}–O^{2-} pairs and shift MO adsorption mode

Table 3
Effect of the reaction atmosphere on the gas-phase HTR of mesityl oxide with 2-propanol

Catalyst	Atmosphere	Conversion[a] (%)		Selectivities[a] (%)						
		X_{MO}	X_{2P}	UOL	*i*-MO	MIBC	MIBK	MIBK/MIBC	AC	Others
MgO	N_2	71.3	15.9	39.0	26.0	26.1	0.8	0.03	4.5	3.6
	H_2	71.5	17.2	36.7	30.2	20.8	6.4	0.3	1.7	4.2
$MgAl_{0.33}O_x$	N_2	90.9	23.8	4.0	5.8	25.0	33.6	1.3	31.3	0.3
	H_2	90.8	23.4	3.6	5.5	24.0	37.4	1.6	29.5	0.0
$Cu_{0.05}MgAl_{0.65}O_x$	N_2[b]	96.0	82.7	0.0	1.6	3.4	68.0	20.0	27.0	0.0
	H_2	99.9	83.7	0.0	0.0	7.4	57.3	7.7	35.3	0.0

T = 523 K; $N_2(H_2)$/2P/MO = 93.4/6.6/1.3 kPa; W/F^0_{MO} = 15 g h/mol.
[a] At t = 0.
[b] W/F^0_{MO} = 10 g h/mol.

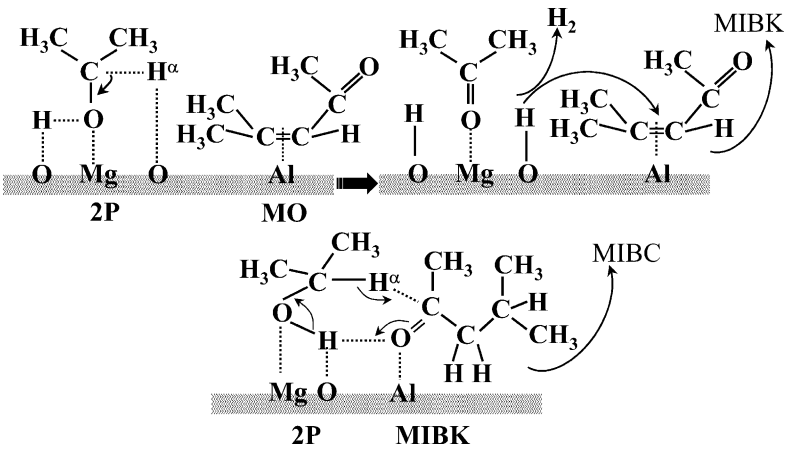

Scheme 4. Gas-phase HTR of MO with 2P on $MgAl_{0.33}O_x$. MIBK and consecutive MIBC formation.

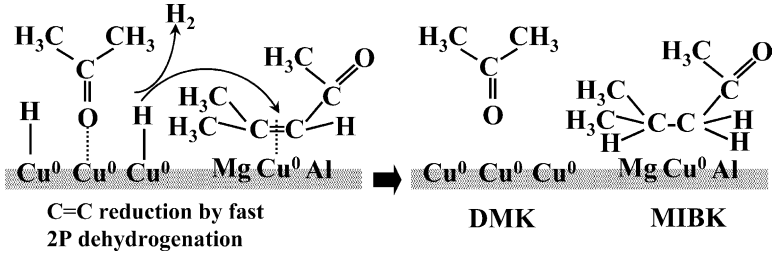

Scheme 5. Gas-phase HTR of MO with 2P on $Cu_{0.05}MgAl_{0.65}O_x$. MIBK formation.

favoring the fast HTR of the C=C bond. Surface Lewis acid Al^{3+} cations also favor DMK and MO polymerization to AC compounds. Ivanov et al. [12] showed that HTR on Lewis acid catalysts is affected by competitive aldol condensation reactions since ketone adsorption under flow conditions probably displaces coordinated alcohol adsorption leading preferentially to AC products.

On $Cu_{0.05}MgAl_{0.65}O_x$ catalyst, surface Cu^0 atoms readily decompose 2P (Fig. 3A) forming acetone and mobile surface H fragments that migrate to selectively reduce the C=C bond of MO giving MIBK, as depicted in Scheme 5. In fact, we obtained similar results in a previous work on MIBK synthesis from 2-propanol on bifunctional Cu-based catalysts [18]. Scheme 5 is indeed similar to Scheme 4 because metal cations of the $MgAl_{0.33}O_x$ catalyst and copper metal atoms of the $Cu_{0.05}MgAl_{0.65}O_x$ catalyst promote the same reaction pathway toward MIBK. However, whereas MO conversion rates are comparable on both catalysts, 2P dehydrogenation rate on $Cu_{0.05}MgAl_{0.65}O_x$ is much faster than on $MgAl_{0.33}O_x$ (Table 2). In fact, we measured a r^0_{2P} = 2225 μmol/(h m^2) on $Cu_{0.05}MgAl_{0.65}O_x$ in contrast to 800 μmol/(h m^2) on $MgAl_{0.33}O_x$. As a consequence of the higher surface hydrogen pressure, reduction of the C=C bond is two-fold faster on $Cu_{0.05}MgAl_{0.65}O_x$ ($r^0{}_{MIBK}$ = 683 μmol/(h m^2)) than on $MgAl_{0.33}O_x$ ($r^0{}_{MIBK}$ = 296 μmol/(h m^2)).

In spite of the higher concentration of surface-generated hydrogen fragments, MIBC is obtained in smaller concentrations on $Cu_{0.05}MgAl_{0.65}O_x$ (Fig. 3B) than on $MgAl_{0.33}O_x$ (Fig. 4B) because it is formed via different reaction pathways on both samples. In fact, on $Cu_{0.05}MgAl_{0.65}O_x$ MIBC formation from MIBK hydrogenation is hindered because thermodynamics but also because of insufficient surface hydrogen concentration generated by 2P dehydrogenation. The latter explains the positive effect of the hydrogen pressure in forming MIBC at expenses of MIBK compared to the typical experiment in N_2 (Table 3). In contrast, on $MgAl_{0.33}O_x$ MIBC is essentially formed by HTR of MIBK with 2P according to Scheme 4, and the presence of H_2 in gas phase does not change significantly the MIBC yield (Table 3).

4. Conclusions

The rates and product distributions for the hydrogen transfer reduction of mesityl oxide with 2-propanol on Mg-based catalysts greatly depend on the ability of surface active sites for promoting both the coordination of adjacent adsorbed reactants and the selective promotion of C=O or C=C bonds in the adsorbed mesityl oxide molecule.

Bifunctional $Cu_{0.05}MgAl_{0.65}O_x$ catalyst combine metal and acid–base sites for producing predominantly MIBK. Copper metal atoms readily dehydrogenate 2-propanol to acetone forming significant amounts of dissociated hydrogen which migrates then from Cu^0 atoms to selectively hydrogenate the C=C bond of mesityl oxide adsorbed on either surface Cu^0 atoms or $Mg^{2+}(Al^{3+})$–O^{2-} acid–base sites of

the support. The $MgAl_{0.33}O_x$ sample combines metal cations of different electronegativities which promote both C=C and C=O reductions giving mainly C_6 and C_9 saturated ketones and alcohols. Lewis acid Al^{3+} cations adsorb mesityl oxide via a π_{C-C} complex of the C=C bond thereby promoting its selective hydrogenation to MIBK with hydrogen fragments generated from 2-propanol dissociation on surface Mg^{2+}–O^{2-} or Al^{3+}–O^{2-} pairs. MIBK is then consecutively transformed to MIBC and C_9 aldol condensation products, which are formed in significant amounts at high mesityl oxide conversions. In contrast, formation of the allyl alcohol from mesityl oxide is not significant on $MgAl_{0.33}O_x$, even for total conversion of mesityl oxide.

MgO selectively reduces mesityl oxide to the allyl alcohol at unusually high yields for a gas-phase reaction. The unique performance of MgO is based on the ability of weak acid–strong base Mg^{2+}–O^{2-} pair sites for promoting formation of the six-atom cyclic intermediate needed in Meerwein–Ponndorf–Verley mechanism for preferentially transferring hydrogen from the 2-propanol donor molecule to the C=O bond of mesityl oxide. In fact, mesityl oxide adsorbs via the C=O bond on a weak Lewis acid Mg^{2+} cation, whereas 2-propanol adsorbs non-dissociatively on a vicinal Mg^{2+}–O^{2-} pair, giving rise to the required bimolecular six-atom cyclic intermediate. The hydride transfer occurs then selectively toward the allyl alcohol without participation of surface H fragments from 2-propanol dissociation.

Acknowledgments

Authors thank CONICET, Argentina (Grant PIP 02933/00) and the Universidad Nacional del Litoral (UNL), Santa Fe (CAI + D 200017-1-47) for the financial support of this work and Dr. V.K. Díez for technical assistance.

References

[1] P. Gallezot, D. Richard, Catal. Rev. -Sci. Eng. 40 (12) (1998) 81.
[2] A.J. Marchi, D.A. Gordo, A.F. Trasarti, C.R. Apesteguía, Appl. Catal. A: Gen. 249 (2003) 53.
[3] C.F. de Graauw, J.A. Peters, H. van Bekkum, J. Huskens, Synthesis (1994) 1007.
[4] V. Ponec, Appl. Catal. A: Gen. 149 (1997) 27.
[5] M. von Arx, T. Mallat, A. Baiker, J. Mol. Catal. A: Chem. 148 (1999) 275.
[6] C. Milone, R. Ingoglia, M.L. Tropeano, G. Neri, S. Galvagno, Chem. Commun. (2003) 868.
[7] E.J. Creyghton, S.D. Ganeshie, R.S. Downing, H. van Bekkum, J. Mol. Catal. A: Chem. 115 (1997) 457.
[8] M.A. Aramendia, V. Borau, C. Jimenez, J.M. Marinas, A. Porras, F.J. Urbano, Appl. Catal. A: Gen. 172 (1998) 31.
[9] J. Lopez, J. Sanchez Valente, J.M. Clacens, F. Figueras, J. Catal. 208 (2002) 30.
[10] A. Corma, M.E. Domine, S. Valencia, J. Catal. 215 (2003) 294.
[11] S.H. Liu, S. Jaenicke, G.K. Chuah, J. Catal. 206 (2002) 321.
[12] V.A. Ivanov, J. Bachelier, F. Audry, J.C. Lavalley, J. Mol. Catal. 91 (1994) 45.
[13] T.M. Jyothi, T. Raja, B.S. Rao, J. Mol. Catal. A: Chem. 168 (2001) 187.
[14] J. Kaspar, A. Trovarelli, F. Zamoner, E. Farnetti, M. Graziani, in: M. Guisnet (Ed.), Heterogeneous Catalysis and Fine Chemicals II, Elsevier Science, Amsterdam, 1991, p. 253.
[15] M.A. Aramendia, V. Borau, C. Jimenez, A. Marinas, J.M. Marinas, A. Porras, F.J. Urbano, Catal. Lett. 50 (1998) 173.
[16] G. Szollosi, M. Bartok, J. Mol. Catal. A: Chem. 148 (1999) 265.
[17] J.I. Di Cosimo, V.K. Díez, C.R. Apesteguía, Appl. Catal. A: Gen. 137 (1996).
[18] J.I. Di Cosimo, G. Torres, C.R. Apesteguía, J. Catal. 208 (2002) 114.
[19] J.I. Di Cosimo, V.K. Díez, M. Xu, E. Iglesia, C.R. Apesteguía, J. Catal. 178 (1998) 499.
[20] V.K. Díez, C.R. Apesteguía, J.I. Di Cosimo, J. Catal. 215 (2003) 220.
[21] S. Fifniades, A.B. Levy, Ullmann's Enclyclopedia of Industrial Chemistry, sixth ed., Weinheim, Germany, 2002 (electronic release).
[22] H. Hattori, Appl. Catal. A: Gen. 222 (2001) 247.
[23] N. Ravasio, M. Antenori, M. Gragano, P. Mastrorilli, Tetrahedron Lett. 37 (1996) 3529.
[24] I.M. Klotz, R.M. Rosenberg, Chemical Thermodynamics: Basic Theory and Methods, sixth ed., J. Wiley and Sons, New York, 2000.
[25] M.G. Musolino, P. De Maio, A. Donato, R. Pierpaolo, J. Mol. Catal. A: Chem. 208 (2004) 219.
[26] S.R. de Miguel, M.C. Román-Martinez, D. Carzola-Amorós, E.L. Jablonski, O.A. Scelza, Catal. Today 66 (2001) 289.
[27] G. Szollosi, M. Bartok, Appl. Catal. A: Gen. 169 (1998) 263.
[28] G. Szollosi, M. Bartok, Catal. Lett. 59 (1999) 179.
[29] J.I. Di Cosimo, C.R. Apesteguía, M.J.L. Ginés, E. Iglesia, J. Catal. 190 (2000) 261.
[30] F. Delbecq, P. Sautet, J. Catal. 152 (1995) 217.
[31] M.A. Aramendía, V. Borau, C. Jimenez, J.M. Marinas, J.R. Ruiz, F.J. Urbano, Appl. Catal. A: Gen. 255 (2003) 301.
[32] P.S. Kumbhar, J. Sanchez-Valente, J. Lopez, F. Figueras, Chem. Commun. (1998) 535.